JOURNAL OF MATERIALS SCIENCE 13 (1978) 1303–1310

The formation of chromium carbide during chromizing

A. J. PERRY, E. HORVATH
Berna AG, Bernex Division, CH-4600 Olten, Switzerland

The carbides formed during the chromizing of various types of carbon and chromium steels are considered in terms of the ternary phase diagram. A correlation is found between the carbide or carbides formed and a diffusion couple model. In low chromium, high carbon steels, an intermediate layer is formed which seems to be a $(Fe,Cr)_3C$ cementite phase. The carbide which is formed on low carbon constructional steels depends on the detailed carbon and chromium profiles. Data found in the literature support the present interpretation.

1. Introduction

In the industrial process known as chromizing [1], chromium is carried to the surface of steels containing 0.1 to 0.2% C where a diffusion profile develops with about 50% Cr at the outer surface of the steel. The steel then has the excellent corrosion and heat resistance found in high chrome steel. Depending to some extent on the size of the part concerned and the particular treatment conditions, there is an upper limit of about 0.3% to the tolerable carbon level for chromizing. Beyond this limit a hard chromium carbide layer is formed [2–8] which has relatively poorer corrosion resistance. In practice this tendency to carbide formation can be overcome either by a surface decarburization pre-treatment or by using the so-called IK steels [2, 8] which are compositionally similar to the current high strength low alloy steels.

Chromium carbide is formed on the steel surface as the result of the reaction between the chromium being deposited and carbon diffusing to it from the steel substrate itself [2–8]. The carbide grows outwards (in contrast to the chromizing diffusion profile) and its continued growth is controlled by the diffusion of carbon through the carbide which acts as a barrier to the inward chromium diffusion [9]. The carbide-forming process is thus diffusion controlled and can be likened to a diffusion couple between chromium and steel at the chromizing temperature. In the present work some experimental data from chromizing by chemical vapour deposition (CVD) are combined with results drawn from the literature to show that the surface coating and the general metallographic features can be described in terms of the iron–chromium–carbon phase diagram. The microstructures concerned are largely independent [10] of the chromizing process used; either pack-cementation [2–8, 10–12] or CVD [10, 13–15]. It is worth adding that the surface finish tends to differ, being matt in the former [12] and invariably smooth and glossy in the latter [14, 15].

Technically the carbide layer is hard and wear resistant so that it can be applied to drop forging dies and to tools for cutting and abrading steels and plastics [16]. Another industrial use is in deep drawing punches and dies and in forging applications [11] and the present writers have described an application in roller bearings [14, 15]. The lifetime increase which can be expected varies from $\times 2\frac{1}{2}$ to $\times$ 100 depending upon the particular application [12, 14–16] and corrosion resistance comparable with acid-resisting steels has been claimed [11].

2. Phase diagram considerations

Part of the isothermal section of the iron–chromium–carbon phase diagram at 1000° C is shown in Fig. 1. This temperature was chosen because it is about that used for most chromizing procedures. The diagram was taken from the study of Bunghardt

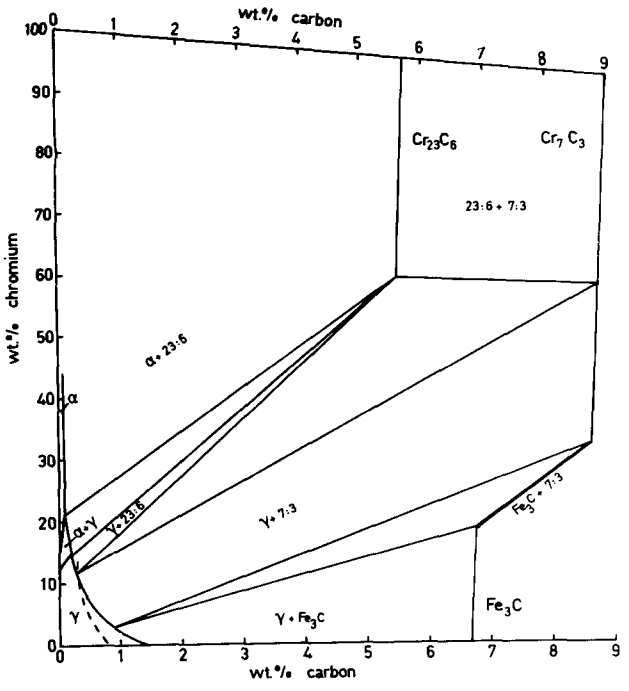

Figure 1 Phase diagram of iron–chromium–carbon alloys at 1000° C showing the Fe–Fe_3C–Cr_7C_3–Cr region.

et al. [17] and is extended to cover the Fe–Fe_3C–Cr_7C_3–Cr section following the summary of earlier work given by Houdremont [18]. Historically the first major study had been that of Tofaute *et al.* [19] which forms the basis of Fig. 1, but which had erred in assuming that the Fe_3C and Cr_7C_3 phases form a direct equilibrium with a miscibility gap on their common tie-line. Dannöhl [20] corrected this situation using data from Heczko [21] for carbides extracted from a wide array of steels. Further studies have since been carried out [17, 22–24] to confirm the form of the diagram and these also show that the carbides remain more or less stoichiometric.

If the greater thermodynamic stability of Cr_7C_3 over $Cr_{23}C_6$ (referred to as 7 : 3 and 23 : 6 hereafter) and the composition of the steel substrate are taken into account, then the probable diffusion path in a chromium versus steel diffusion couple can be assessed using the phase diagram. Kinetic effects must also be borne in mind because the presence of both chromium and carbon in solution in steels reduce their respective diffusional mobilities. Referring to Fig. 1, it is possible to isolate four types of diffusion path behaviour:

(a) high Cr, low C steels which come into equilibrium with a 23 : 6 layer only.

(b) high Cr, high C steels where the carbide is expected to be 7 : 3 with possibly an outer layer of 23 : 6.

(c) low Cr, high C steels: as in (b) but with a Fe_3C-based cementite phase located between the 7 : 3 and the substrate.

(d) low Cr, low C steels where chromium enrichment of the substrate during chromizing (possibly with decarburization) can lead to a surface concentration in the γ-phase which comes into equilibrium with 23 : 6 or 7 : 3 as seen in Fig. 1.

The four types correspond to four distinct classes of commercial steels:

(a) 13% Cr, low C chemically resistant steels.

(b) 12% Cr, 2% C tool steels.

(c) low Cr, C ⩾ 0.8% low chrome tools steels, wear resistant and roller bearing steels.

(d) some class (c) steels of lower carbon content and also the carbon and low chromium constructional steels.

3. Experimental

A series of commercial steels was chromized in an industrial CVD installation [15] under conditions designed to produce 7 : 3 on the surface of a 1.5% Cr, 1% C steel [14]. The steels included the four classes described above as shown by the series of symbols in Fig. 2.

All the samples were examined metallographically; in all cases the substrates were etched with a 5% nital solution and the carbide layers with Murakami's reagent. The distribution of Fe, Cr and

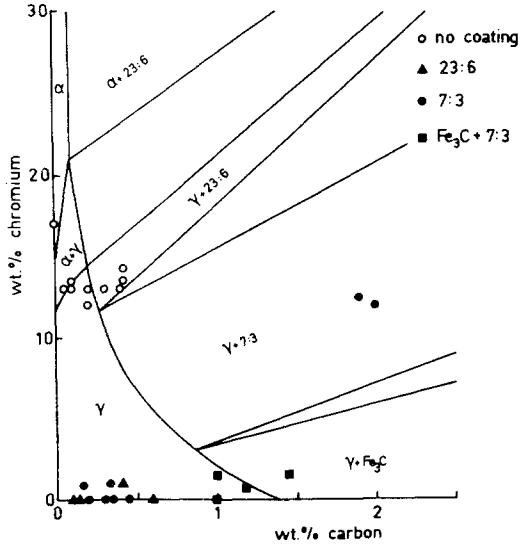

Figure 2 Iron-rich corner of the iron-chromium-carbon phase diagram at 1000° C showing the compositions of the various steels studied here and the type of carbide coatings found on them after CVD chromizing.

C was determined in some samples by electron probe microanalysis (EPMA). The Vickers microhardness of each coating was determined (taken as the average of five readings) and, finally, some fractured samples wer examined in a Camebax scanning electron microscope (SEM) which also included the EPMA facility.

4. Results and discussion

The optical microstructures of the four classes of steel are typified by those given in Figs. 3a to d. They can be discussed as follows:

4.1. High Cr, low C steels

These show no microstructural changes (Fig. 3a) and there is indeed no change in chemical composition at the surface – according to an EPMA scan – with neither chromium absorption nor carbide formation following the present chromizing treatment. There is some surface roughening caused through chemical attack by the HCl produced during the chromizing process [15].

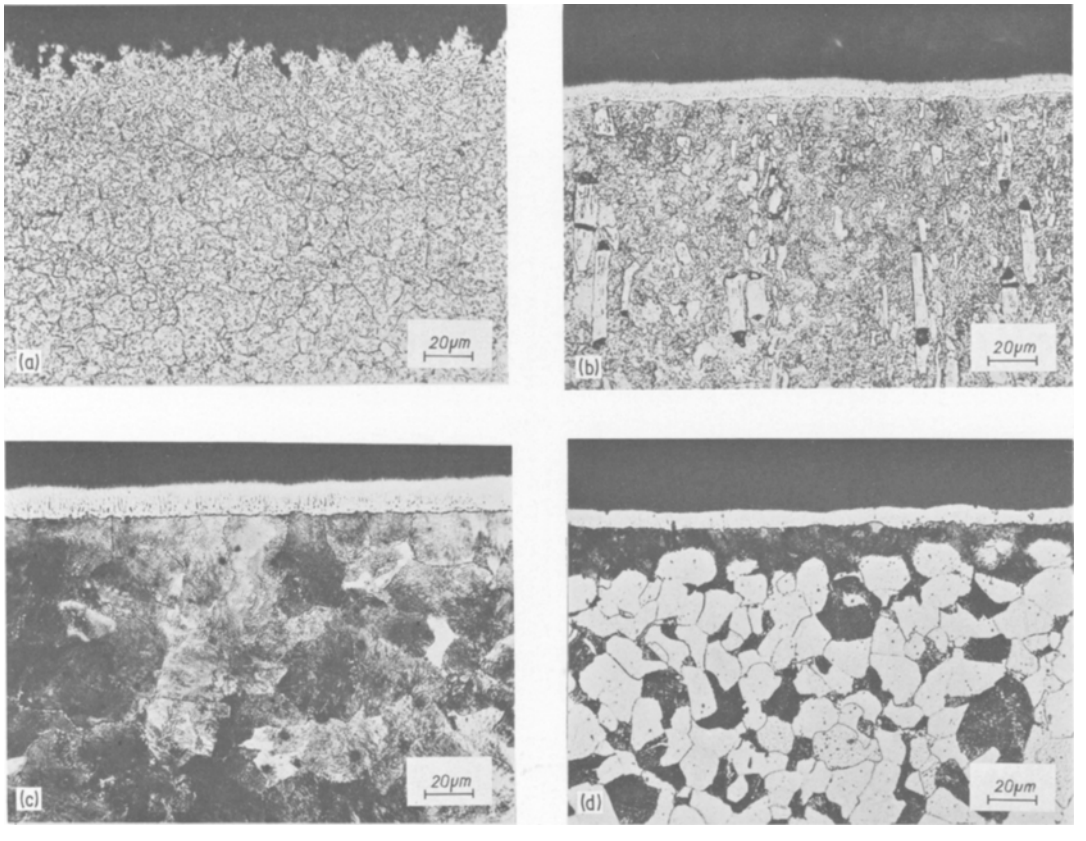

Figure 3 Typical micrographs after CVD chromizing the four classes of steels studied: (a) high Cr, low C steel (DIN 1.4045; 13.5% Cr, 0.42% C); (b) high Cr, high C steel (DIN 1.2080; 12.0% Cr, 2.0% C); (c) low Cr, high C steel (DIN 1.3505, 1.5% Cr, 1.0% C); (d) low Cr, low C steel (DIN Ck45, 0.45% C).

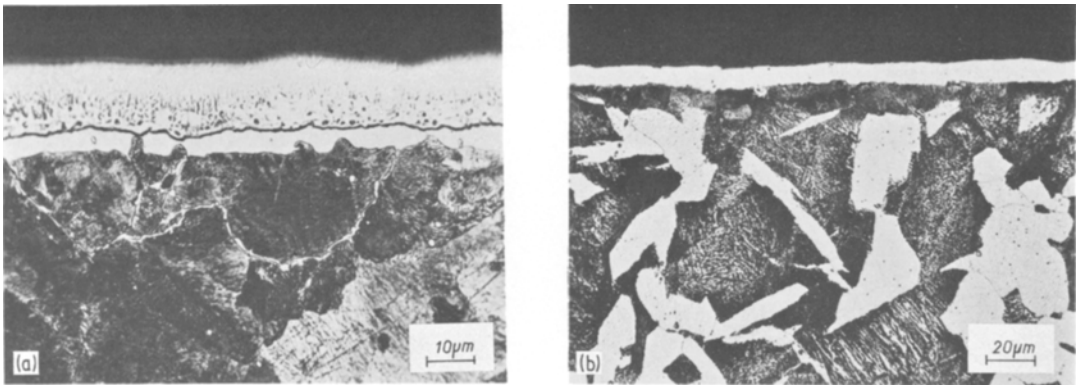

Figure 4 Optical micrographs after CVD chromizing: (a) DIN 1.2063; 1.5% Cr, 1.45% C steel; (b) DIN Ck60; 0.60% C steel.

4.2. High Cr, high C steels

These show (Fig. 3b) a single layer of a fine columnar carbide which was shown [13] to be of the 7 : 3 type.

4.3. Low Cr, high C steels

Steels of composition beyond the binary eutectoid point (which is also approximately the lower limit of the γ-Fe_3C equilibrium phase boundary as seen in Fig. 1) show two distinct layers in the coating (Figs. 3c and 4a). An EPMA scan confirmed that the coating consisted of two layers of different composition; the results are shown in Fig. 5. The iron scan shows a distinct step at the junction between the two layers (allowing for a beam width of 1 μm); the expected [12] steady fall of the iron concentration and increase in the chromium concentration towards the carbide surface can also be clearly seen. It is difficult to analyse for carbon and the electronic noise is too high, so that it is not clear whether the carbon level is different between the two layers. The scan does show a carbon enrichment profile in the steel substrate itself increasing towards the carbide coating.

The outer layer is 7 : 3 [14] with a fine columnar structure and sometimes with a coarser inner region in some higher carbon samples (Fig. 4a). It can be noted in passing that the etch attack decreases as the chromium content of the carbide increases. The intermediate layer is non-etching and apparently featureless. The optical micrograph in Fig. 4a shows that this layer and the intergranular cementite of the substrate are a continuous phase. It is too thin for detailed analysis but the present results are interpreted as showing that it is a $(Fe, Cr)_3C$ cementite phase. The phase boundaries of the two carbide phases are sufficiently close in the phase diagram (Fig. 1) to account for the difficulty in separating them analytically by EPMA alone.

The puzzling feature of the results is the apparently very high carbon level in the substrate at the interface with the carbide layer (Fig. 5) shown by EPMA. The curve would seem to show that the concentration in the substrate rises to about half that in the carbide layer, or about some 3.5%. As the data have not been corrected for absorption effects etc., they cannot be considered to be quantitative and a more complete analysis is in hand. However, there is also a change in the fracture behaviour of the substrate (Fig. 6a) from intercrystalline to transcrystalline which occurs in parallel with the apparently increasing carbon level. In contrast, the optical and scanning micrographs (Figs. 3c, 4 and 6b) show no apparent differences in microstructures throughout the samples. They remain simple uniform hypereutectoid structures with a small amount of intergranular carbide corresponding to single phase γ-austenite at the chromizing temperature. One explanation might have been graphitization but there is no sign of it. It should be added that such effects were not found in any other steels in this class (low Cr, high C) so that some influence of a pre-treatment step may be responsible in this particular case.

4.4. Low Cr, low C steels

These show a single carbide layer and an associated increase in the pearlite concentration. This apparent increase can also be discerned in micrographs in the literature [5–9].

In the alloys of types (b) and (c) which were

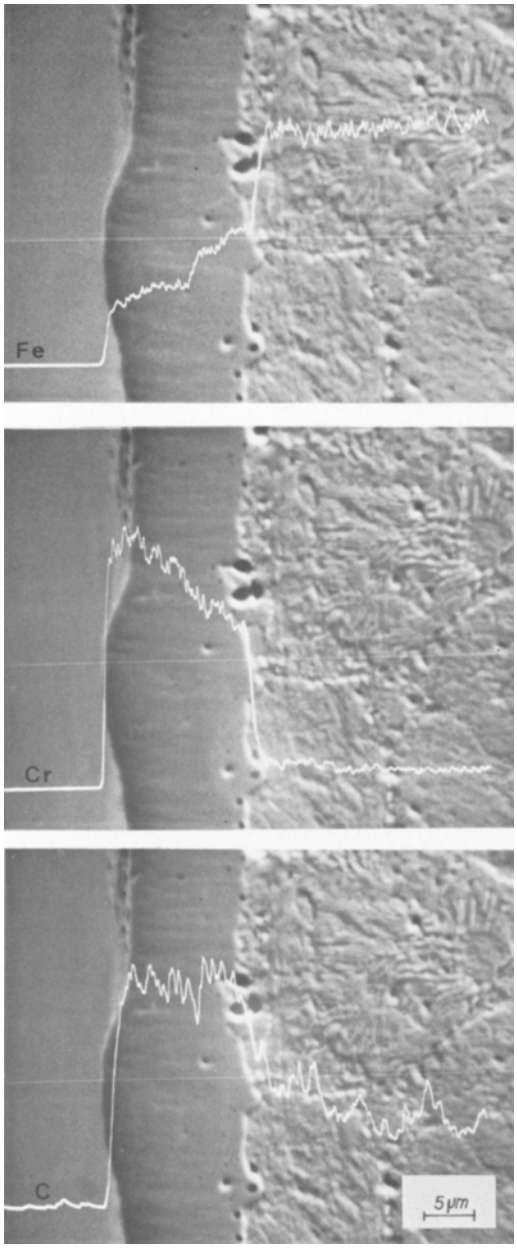

Figure 5 Electron probe microanalyser scans for the elements Fe, Cr and C across a sectioned 1.5% Cr, 1.0% C steel after chromizing.

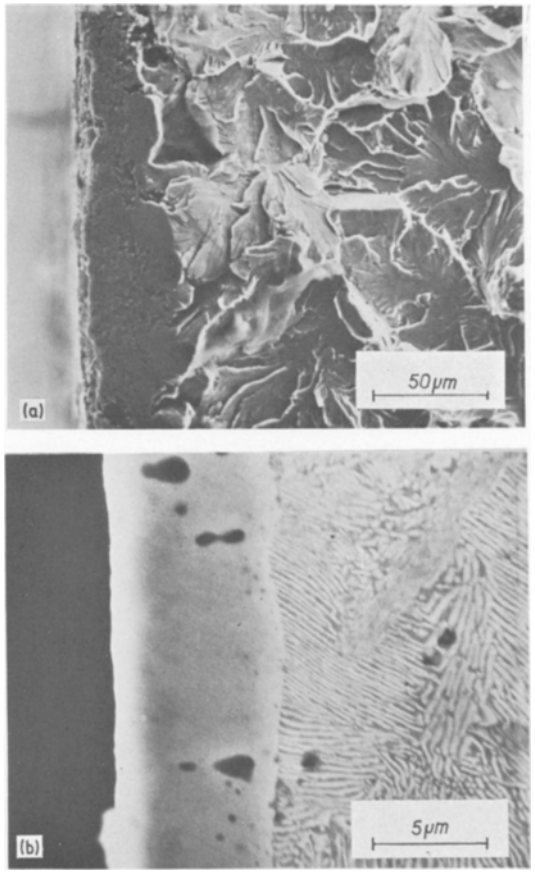

Figure 6 Scanning electron micrographs: (a) a fractured sample of a 1.5% Cr, 1.0% C steel after chromizing; (b) a polished and etched section of the same steel after chromizing.

discussed in Sections 4.2 and 4.3 above, the composition of the γ-phase in the substrate during the chromizing process corresponds in most cases to the γ-phase boundary solid solution limit, so that chromium is not absorbed (Fig. 5) by the austenite. The situation is different in the type (d) alloys discussed in this section; chromium is first absorbed as a diffusion profile. The concentration at the surface has to increase to the γ solid solution phase boundary level before any carbide can form. The precise chromium profile and the diffusion profile of carbon moving in the reverse direction (to form carbide or due to decarburization) control the precise compositions at the surface of the steel, the point on the γ solid solution phase boundary which is reached and hence (as can be seen by reference to Fig. 2) the nature of the carbide which is then formed i.e. the 23:6 or 7:3 type. The associated increase in the pearlite can also be understood in these terms: The dashed curve in Fig. 1 indicates the shift in the eutectoid composition to lower carbon concentrations with increasing chromium [19]. It is also interesting to note that at 1000° C it intersects the γ-phase boundary between the 23:6 and 7:3 equilibria phase field, so that a eutectoid or hypereutectoid layer should always be found in the substrate below the 7:3 carbide, as seen in Fig. 3d. It should be added that this type of argument also differen-

tiates the high carbon steels which form the intermediate cementite layer from those which do not: Chromizing steels containing more than 0.9% C cause the composition of the γ-phase at the steel surface to intersect the γ-Fe_3C phase boundary so that cementite forms first. As remarked above, this composition is also approximately the binary eutectoid. In lower carbon steels the γ-Cr_7C_3 phase boundary is intersected so that no cementite is formed as an intermediate layer.

5. Microhardness measurements

The microhardness values $H_v^{0.025}$ of the carbide coatings and the unchromized substrates for the type (a) alloys of Section 4.1 are shown in Fig. 7a as a function of the carbon level of the substrate. The tool steels are known to be coated with 7:3 carbide [13] and the outer layer of the coating on the 1.5% Cr, 1.0% C steel is similarly known to be 7:3 [14]. The nature of the other coatings is not known. The purpose of the microhardness measurements was to correct this by identifying the phases through their hardness values.

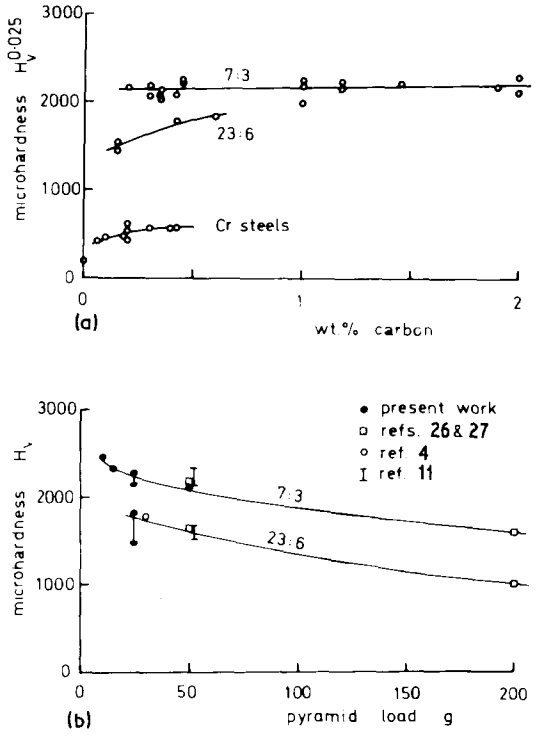

Figure 7 Vickers microhardness values: (a) of the present carbide coatings and high chromium steels as a function of the carbon content of the steels together with the present interpretation; (b) a comparison of the present results with published values as a function of the pyramid load.

The variation of the microhardness with the pyramid load is shown in Fig. 8a. This has been interpreted in terms of elastic relaxation [25]. Assuming a constant relaxation of 0.24 μm in the length of the indent diagonal (Fig. 8b), a macroscopic hardness of 2030 kg mm^{-2} for the 7:3 carbide can be derived. In addition, the minimum coating thickness necessary for microhardness measurements can be given as a function of the pyramid load (dash-dot curve shown in Fig. 8b). It should be noted that the highest load of 50 g requires a minimum thickness of 15 μm; the sample used for this study had a particularly thick coating of 20 μm. A comparison with published data [26, 27] is given in Fig. 7b as a function of the pyramid load for both the 7:3 and the 23:6 carbides.

Accepting the rough-and-ready nature of the analysis, the present interpretation is shown in Fig. 7a and is included in Fig. 2. The high carbon

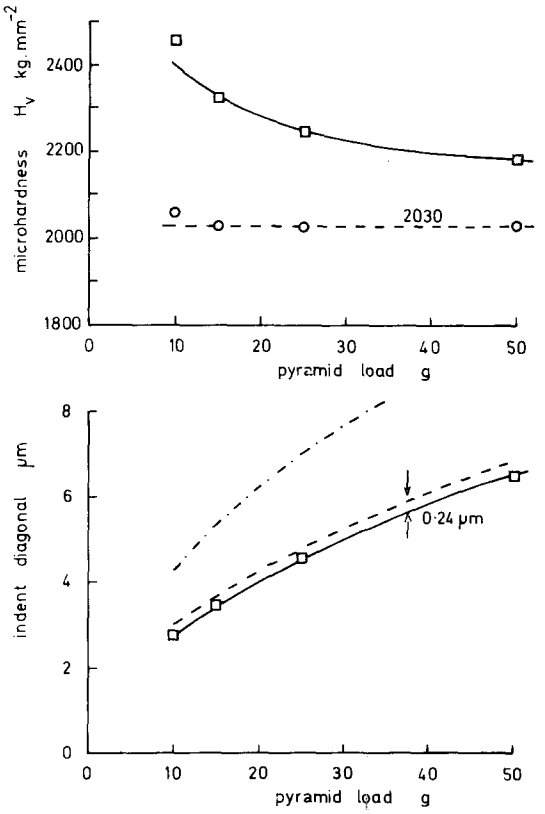

Figure 8 Vickers microhardness values, as a function of the pyramid load, of the $(Cr, Fe)_7C_3$ coating formed on a 1.5% Cr, 1.0% C steel after chromizing. Also shown is the analysis of the indent diagonal length assuming an elastic relaxation [25] of 0.24 μm (dashed curve) to give the microhardness of 2030 kg mm^{-2}. The dash-dot curve is the minimum coating thickness required for measurements [25] as a function of pyramid load.

steels (types (b) and (c)) correspond with 7:3 as expected, showing that its hardness is independant of the substrate composition in all the present steels. The low carbon steels show some 23:6 carbide layers in an apparently irregular fashion. This is attributed to the detailed carbon and chromium profiles as discussed above. It was not expected, for example, that the 0.6% C steel would develop a 23:6 coating. However, the sample must have had a degree of surface decarburization because the structure of the substrate shows primary ferrite both just below the coating and throughout the sample (Fig. 4b). Following earlier discussion this also would point to a surface composition consistent with a 23:6 carbide to have developed during chromizing.

It should be added that the analogy with a diffusion couple shows that a 23:6 carbide, once formed, will not develop a 7:3 outer layer during chromizing. In contrast a 7:3 layer can be expected to develop 23:6 carbide on its outer surface depending on the rates of arrival of chromium from the gas phase and of carbon diffusing through the carbide from the substrate.

The carbide sequence of all the samples is indicated in Fig. 2 where a comparison with the phase diagram is possible. The present data are too limited to allow definite conclusions to be drawn but they appear to indicate a general correlation between the phase diagram, the diffusion couple model and the structures observed here.

6. Comparison with existing results

As quoted above, Hänni and Hintermann [13] identified the carbide on tool steels as 7:3 type. The hardness value $H_v^{0.03}$ of 1800 kg mm^{-2} reported by Samuel *et al.* [4] appears to correspond to the 23:6 carbide according to the data assembled in Fig. 7b. The diffusion couples studied by Monnier *et al.* [12] are nearly all in accordance with the present study. They analysed the layers chemically and the findings are shown in Table I. The exception is the last case where an intermediate cementite layer on the substrate would be expected. It is possible that such a layer was too thin for analysis or that the nearness of the phase

TABLE I

Substrate	Layers
High Cr, low C steel	23:6
Medium carbon steel	7:3, 23:6
High carbon steel	7:3, 23:6

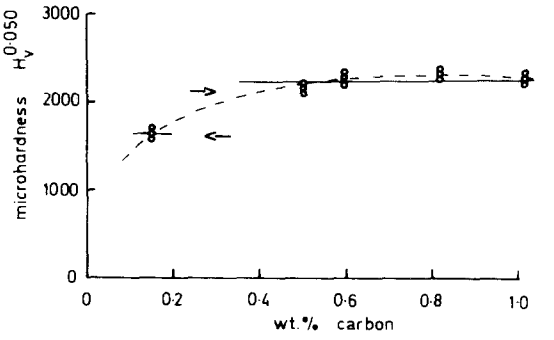

Figure 9 Vickers microhardness data of Cseh [11] showing his interpretation (dashed curve), the present interpretation (full curve), with the arrows representing the microhardness values interpolated from Fig. 7b.

boundaries created the analytical problems also encountered here.

Cseh [11] reported the microhardness values $H_v^{0.050}$ shown in Fig. 9 as a function of substrate carbon level. Interpolating the data in Fig. 7b to produce the arrow values shown in Fig. 9, the present work indicates the carbide on the 0.15% C substrate to be 23:6 whilst the remaining samples were coated with the 7:3 type carbide. Cseh interpreted the data as a steady variation of hardness (dashed curve) with substrate composition; the present work indicates a stepped curve (full curve in Fig. 9), corresponding to the change in nature of the carbide.

Finally, the recent extensive study of Tacikowski *et al.* [10] is particularly relevant. They studied the nature of the carbide layer sequence in a series of plain carbon steels chromized both by CVD and pack-cementation processes. The results (with the exception of an outer nitride layer caused by trapped air in their pack process) were the same for both processes and follow the sequences expected here including the outer 23:6 layer on 7:3 carbide coatings. They also report the existence of an unidentified non-etching intermediate layer in hypereutectoid steels which we believe to be cementite. The coarser structured inner layer in the 7:3 coating (Fig. 4a) on high carbon steels was extensively studied by them and attributed to compositional effects: the mode of growth changes at a certain chromium level.

7. Conclusions

A series of commercial steels has been chromized using an industrial CVD process. The microstructure and microhardness of the carbide layers formed was studied and it was found that the

majority of samples formed a $(Cr, Fe)_7C_3$ carbide coating. Some low Cr, high C steels form an intermediate layer which appears to be cementite $(Fe, Cr)_3C$.

The present work is far from complete and it is clear that the proposed cementite intermediate layer needs a fuller analysis. The use of microhardness measurements alone for phase identification is questionable because the microhardness of carbides is sensitive to crystal orientation [28], to the detailed microstructure [10] and it is possible that columnar structures have similar effects to those found in composite structures [29]. Nevertheless the microhardness values measured here show a remarkable degree of self-consistency in the $(Cr, Fe)_7C_3$ phase, the microstructure of which was practically always a fine columnar one.

The general consistency of the present results and those already published in the literature tends to support the present proposal that the carbide sequence formed on chromizing can be described in terms of phase diagram considerations.

References

1. A. H. SULLY and E. A. BRANDES, "Chromium" (Butterworths, London, 1967) p. 258.
2. R. L. SAMUEL and N. A. LOCKINGTON, *Metal Treatment and Drop Forging* **18** (1951) 440
3. *Idem, ibid.* **18** (1951) 495.
4. R. L. SAMUEL, N. A. LOCKINGTON and H DORNER, *ibid.* **22** (1955) 288.
5. P. GALMICHE, *Rev. Mét.* **47** (1950) 192.
6. G. BECKER, K. DAEVES and F. STEINBURG, *Z. phys. Chem.* **A187** (1940) 354.
7. *Idem, Stahl u. Eisen* **61** (1941) 289.
8. *Idem, Metallwirtschaft* **20** (1941) 217.
9. R. BERNST, *Neue Hütte* **13** (1968) 352.
10. J. TACIKOWSKI, W. LILIENTAL, I. SULKOWSKI and J. TROJANOWSKI, Proceedings of the 5th International Symposium on Metallkunde und Wärmebehandlung 1975, Karl-Marx-Stadt, Paper III/8.
11. S. CSEH, Proceedings of the 1st International Symposium on Metallkunde und Wärmebehandlung, 1967, Warsaw, Paper B12.
12. G. MONNIER, R. RIVIÈRE and M. LASSUS, *C.R. Acad. Sci. Paris* **261** (1965) 4094.
13. W. HÄNNI and H. E. HINTERMANN, *Thin Solid Films* **40** (1977) 107.
14. E. HORVATH and A. J. PERRY, Proceedings of the 9th Plansee Seminar, Reutte 1977, Paper 39.
15. H. E. HINTERMANN, A. J. PERRY and E. HORVATH, *Wear* **47** (1978) 407.
16. R. L. SAMUEL and N. A. LOCKINGTON, *Metal Treatment and Drop Forging* **19** (1952) 81.
17. K. BUNGHARDT, E. KUNZE and E. HORN, *Arch. Eisenhüt.* **29** (1958) 193.
18. E. HOUDREMONT, "Handbuch der Sonderstahlkunde", 3rd edition (Springer-Verlag, Berlin, 1956) p. 623.
19. W. TOFAUTE, C. KÜTTNER and A. BÜTTINGHAUS, *Arch. Eisenhütt.* **9** (1936) 607.
20. W. DANNÖHL, *Stahl u. Eisen* **69** (1949) 85.
21. Th. HECZKO, *Berg u. Hüttenm. Mh.* **92** (1947) 125.
22. E. HOUDREMONT, W. KOCH and H. -J. WIESTER, *Arch. Eisenhütt.* **18** (1945) 147.
23. K. KUO, *J. Iron Steel Inst.* **173** (1953) 363.
24. T. WADA, H. WADA, J. F. ELLIOTT and J. CHIPMAN, *Met. Trans.* **3** (1972) 2865.
25. H. BÜCKLE, "Mikrohärteprüfung und ihre Anwendung" (Berliner Union, Stuttgart, 1965) pp 210, 240.
26. J. HINNÜBER and O. RÜDIGER, *Arch Eisenhütt.* **24** (1953) 267.
27. J. H. WESTBROOK, *J. Metals* **9** (1957) 898.
28. D. J. ROWCLIFFE and G. E. HOLLOX, *J. Mater. Sci.* **6** (1971) 1261, 1270.
29. A. J. PERRY and D. J. ROWCLIFFE, *ibid.* **8** (1973) 904.

Received 30 September and accepted 1 November 1977.